Journal of Applied Polymer Science

Evaluation of polymer hydrophobic recovery behavior following H_2O plasma processing

Brendan D. Tompkins, Ellen R. Fisher
Department of Chemistry, Colorado State University, Fort Collins , Colorado , 80523-1872
Correspondence to: E. R. Fisher (E-mail: erfisher@lamar.colostate.edu)

ABSTRACT: Inductively coupled radio frequency (rf) H_2O vapor plasma was used to modify a range of polymers to better elucidate the dependence of hydrophobic recovery on polymer composition and structure. Freshly modified and aged samples were examined using scanning electron microscopy, (SEM), X-ray photoelectron spectroscopy, (XPS), and water contact angle (wCA) goniometry. Initially, wettability was increased on each polymer surface due to the implantation of polar oxide groups, an effect exacerbated by increased surface roughness with plasma treatment. Polypropylene and polystyrene exhibit nearly complete hydrophobic recovery as polar groups are subsumed as samples age. High-density polyethylene and polycarbonate exhibit minimal hydrophobic recovery, owing to plasma-induced cross-linking and intrinsic thermal stability, respectively. Overall, the hydrophobic performance following H_2O plasma modification is similar to other oxidizing plasmas, suggesting that recovery behavior is intrinsic to the polymer. © 2015 Wiley Periodicals, Inc. J. Appl. Polym. Sci. **2015**, *132*, 41978.

KEYWORDS: aging; hydrophilic polymers; polycarbonates; polystyrene; surfaces and interfaces

Received 27 August 2014; accepted 16 January 2015
DOI: 10.1002/app.41978

INTRODUCTION

Polymers find extensive use in many important modern industries, including automotive,[1,2] biomedical,[3,4] environmental,[5] and laboratory applications.[6] Often, however, the properties of the polymer surface, including surface tension and surface functionality, are incompatible with the intended application, thereby limiting their utility. Among the most common issues, adhesive failure and delamination are resulting from interface incompatibility,[1,7–9] wetting and fouling issues arising from undesirable surface tension or surface functionality,[10–15] and surface instability causing the polymer surface to denature or degrade.[2] Each of these issues can be mitigated by surface modification processes, including exposure to ultraviolet radiation,[16,17] flame treatment,[18] and plasma surface modification.[19,20] Indeed, plasma surface modification of polymers has a long history[21–23] in part from the many plasma techniques and chemistries available, and the inherit ability to limit the modification only to the outermost layer of a polymer material.[19] Unfortunately, many of these polymer surface modifications lack permanence and are unstable, resulting in polymer surfaces reverting back to their untreated states over time, which is referred to as aging or hydrophobic recovery.[20]

As outlined by Truica-Marasescu *et al.*[17] and Pascual *et al.*,[24] postulated theories on processes contributing to polymer aging and hydrophobic recovery include the following: (1) adsorption of nonpolar contaminates such as carbon to the surface; (2) long-range reorganization, including the diffusion of oligomers and additives to the surface;[25] (3) short-range reorganization, including the reorientation of the polymer to present a lower energy surface;[25] and (4) the diffusion of low molecular weight oxidized material (LMWOM) beneath the polymer surface. Overall, researchers have made strides toward understanding the aging process on polymer surfaces leading to a model that accurately predicts the rate and extent of hydrophobic recovery.[26] Despite the strength of such models, however, there is little agreement on the techniques or conditions that yield the most desirable surface modification outcome. Or rather, the literature demonstrates that there is no single best strategy, and the surface modification technique, polymer, and application must be considered collectively.

Preventing polymer surface aging is of particular importance for porous polymer membranes, which are ubiquitous in biomedical applications,[27] gas separations,[28,29] and the purifications of liquids such as water and dairy products.[15,29–32] Fisher and coworkers have a long history of membrane modification using oxidizing inductively coupled radio frequency (rf) plasmas. This research demonstrated that H_2O plasmas implant hydrophilic functionality on the surface of asymmetric PSf membranes used

Additional Supporting Information may be found in the online version of this article.

for many filtration applications,[33] with the goal of achieving a membrane with increased wettability for the purpose of decreasing protein fouling while maintaining or improving selectivity. The study found that the optimal conditions for rendering PSf membranes completely wettable consisted of a 2-min treatment time, applied rf power (P) = 25 W, and 50 mTorr H_2O vapor with the sample oriented perpendicular to the gas flow 9 cm downstream from the coil region. Subsequent studies[34] found that treated surfaces are remarkably stable and remain wettable after 18 months. These results were the impetus for an expanded study[34] that extended the H_2O plasma system to other porous polymer membrane systems, including PES and polyethylene (PE). Each polymer membrane was initially rendered completely wettable following H_2O plasma treatment. In contrast to the persistent wettability on PSf and PES, however, PE exhibited significant hydrophobic recovery. One hypothesis explained the structural and thermal properties of PE make it more susceptible to aging compared to PSf or PES. Indeed, Jokinen *et al.* demonstrated that a range of solid polymers exposed to O_2 or N_2 plasmas will exhibit a range of different aging behaviors. [35] A similar comprehensive study examining H_2O plasma surface modification, however, does not exist.

Here, we investigated the treatment effectiveness of H_2O plasmas and the aging of plasma-modified polymer surfaces using several solid polymer substrates. A wide range of polymers, encompassing different compositions, structures, and physical properties were used in this research, including high-density polyethylene (HDPE), low-density polyethylene (LDPE), polypropylene (PP), polystyrene (PS), and polycarbonate (PC). Cleaned samples are treated using a home-built inductively coupled rf plasma reactor using H_2O vapor as the feed gas and the standard treatment conditions developed previously.[33,34,36] Cleaned control, freshly treated, and aged samples are analyzed using primarily water contact angle (wCA) and X-ray photoelectron spectroscopy (XPS). These results are used to further develop our understanding of how plasma surface modification influences the surface and near-surface polymer structure leading to hydrophobic recovery. Select differential scanning calorimetry (DSC) measurements are also used to ascertain the influence of thermal properties, such as melting temperature (T_m) and glass transition temperatures (T_g), on hydrophobic recovery.

EXPERIMENTAL

Materials and Reagents

The polymer sheets used in this study were HDPE, LDPE, PP, PS, (0.060 in. thickness; United States Plastic Corporation, Lima, OH), and polycarbonate (0.060 in. thickness Lexan® 9034V; Sabic Innovative Plastics, Pittsfield, MA). Specific polymer property details (i.e., molecular weight, PDI, and tacticity) were not available from the manufacturers. Cuttings of each polymer (~1 × 2 cm) were first cleaned by agitating in ethanol (absolute, reagent grade; Mallinckrodt Baker) for 60 s followed by rinsing with ultra-pure H_2O [reverse osmosis (RO) purified, ≥18 MΩ] for 60 s to remove residues from manufacturing and environmental contamination. The washed polymer substrates were then stored in a vacuum desiccator for 24 h before plasma treatment or storage for control samples. Sample sets for plasma treatment and control were prepared concurrently to eliminate any subtle differences in cleaning procedures or storage conditions. To ensure sample analysis was performed on samples not potentially altered by previous analyses, multiple samples were prepared for each time point such that samples were never reused. Ultra-pure H_2O to be used as feed gas for plasma modifications was placed in a side arm vacuum flask and freeze-pump-thawed 3 times to degas prior to use. Ultra-pure H_2O was also used for substrate cleaning and as a probe liquid for wCA measurements without further purification.

H_2O Plasma Modification

H_2O plasma modification was performed in an inductively coupled glass barrel style reactor described previously.[14,37] Briefly, the induction coil is powered by a 13.56 MHz rf power generator (Advanced Energy Industries Inc., Fort Collins, CO) via a matching network, pumping is achieved using a two-stage rotary pump (< 10 mTorr base pressure), and pressure is measured using a Baratron® capacitance manometer (MKS Instruments Inc., Andover, MA). H_2O vapor from a side arm vacuum flask is introduced into the reactor via a needle metering valve. Cleaned polymer substrates were placed at the desired position within the plasma reactor. The reactor was pumped to base pressure and purged with H_2O vapor prior to and following plasma modification. The conditions used (P = 25 W, 50 mTorr, 9 cm downstream substrate position, and 2-min treatment time) were based on previous studies[33,34] and are hereafter referred to as "standard treatment conditions." Fresh control and plasma treated samples were analyzed within 24 h. Aged control and plasma-treated samples were stored in clean PS petri dishes under ambient laboratory conditions, protected from light.

Differential Scanning Calorimetry

The thermal properties of each polymer were measured using differential scanning calorimetry (DSC) using the DSC 2920 (TA Instruments, New Castle, DE). Samples were crimped into hermetically sealed aluminum sample pans, cooled below −100°C, and heated past melting, or up to 250°C in the case of PS, for two full heating cycles at a rate of 10°C min^{-1}. Cooling was aided by a liquid nitrogen cooling system. Analysis of the DSC results was performed using the software provided with the instrument. DSC was only performed on untreated polymer samples because the volume of the modified surface layer on a treated sample would be insignificant compared to the total volume of the bulk sample. Attempting to modify a subsample of a sufficiently small size for DSC would alter the surface area to bulk polymer ratio, rendering any comparison to wCA and XPS results invalid.

Scanning Electron Microscopy

SEM images from untreated and freshly treated samples using the JSM6500F (JEOL, Ltd., Japan) equipped with a field emission source. Samples were prepared by mounting a small cutting (~0.5 × 0.5 cm) onto an aluminum stub using double-sided carbon tape (3 M) and sputter coating with 5 nm of Au to mitigate charging. Samples were imaged using a 6 mm working distance and 5 kV accelerating voltage. HDPE and LDPE

samples were found to be particularly susceptible to thermal damage from the electron beam. Therefore, steps were taken to avoid excessive exposure of the imaged areas to the electron beam prior to collecting images from all samples.

Contact Angle Goniometry

wCA measurements were made under ambient laboratory conditions using the DSA 10 contact angle goniometer (Krüss GmbH, Hamburg, Germany) to characterize changes in wetting behavior with H_2O plasma modification and aging compared to control samples. Still images were taken immediately after dosing a sample with 2 μL of ultra-pure H_2O. The contact angle at the three-phase point was measured by the circle fitting method using the software supplied with the instrument. A minimum of 12 wCA measurements were made for each control and treated sample time point. The reported wCA is the arithmetic mean and error is one standard deviation. The one-month percent wCA recovery was calculated from the mean wCA values based on eq. (1).

$$\%\ \text{Recovery}\ (wCA) = \frac{wCA(1\ \text{Month}) - wCA(\text{fresh})}{wCA(\text{control}) - wCA(\text{fresh})} \times 100\% \quad (1)$$

X-ray Photoelectron Spectroscopy

XPS analysis was performed using the PHI 5800 ESCA system (Physical Electronics, Eden Prairie, MN) equipped with a monochromatic Al Kα source (1486.6 eV, 350.0 W) and a hemispherical electron energy analyzer (survey mode: 187.85 eV pass energy, 0.800 eV resolution; high-resolution mode: 23.5 eV pass energy, 0.100 eV resolution). A low-energy electron flood gun (~5 eV) and argon ion source were used to compensate for surface charging. Each sample was analyzed by first collecting a spectrum in survey mode to identify all elements present. High-resolution mode was then used to collect spectra for each element where the concentration was ≥1%. High-resolution spectra were collected in triplicate from different spots on each sample so that elemental concentration and fitting error could be calculated. Initial processing and calculation of elemental concentrations from the high-resolution spectra were performed using Multipak from Physical Electronics. Each spectrum was smoothed, indexed so that maximum intensity in the C_{1s} region was at 285.0 eV, and baseline corrected using a Shirley function. Elemental concentrations were determined using sensitivity factors supplied with the instrument. The reported concentrations are the arithmetic mean from each sample and the error is one standard deviation.

Deconstruction of the high-resolution C_{1s} spectra was performed using XPSPeak v4.1. All spectra, except those from PS, were fit using a Shirley baseline. PS was fit using a mixed Shirley/linear baseline to compensate for higher background levels arising from the influence of the conjugated π system on the higher energy end of the spectrum where a linear contribution with a slope value of 2.3 gave the most reasonable fit. Initial model C_{1s} spectra were generated based on the following binding environments: allylic carbon (C═C/C═C—H, 284.5 eV), aliphatic carbon (C—C/C—H at 285.0 eV), ether/alcohol (C—O at 286.4 eV), carbonyl (C═O at 287.9 eV), acid/ester (O—C═O at 289.5 eV), and carbonate (O═C(—O)$_2$ at 290.8 eV).[38] The peak positions were constrained by fixing the binding energy (BE) of each oxidized carbon-binding environment (CO_x) peak relative to the C—C/C—H peak. The reduced carbon of PS was fit assuming contributions from aliphatic carbon and allylic carbon and the BE of allylic carbon was not constrained. The full width at half maximum (FWHM) of each component peak was constrained to ≤1.8 eV. All peak shapes were assumed to be 95 : 5 Gaussian/Lorentzian. PS and PC also had significant signals from π–π* shake-up satellites, where the BE and FWHM of the π–π* peak were somewhat variable, ranging from 291.1–292.1 eV and 1.4–2.3 eV, respectively. All peak models were then optimized and adjusted to minimize the χ^2 value. Finally, the raw spectrum, modeled spectrum, and spectral components from each sample were shifted so that the BE of the C—C/C—H component was 285.0 eV. The final peak model from each sample developed from the procedure was applied to the replicate spectra collected from that sample to verify model quality and calculate error for the reported results.

The interpretation of the polyolefin XPS results required a more detailed comparison of C_{1s} and O_{1s} peak areas to differentiate organic oxide from inorganic oxide, in the case of HDPE and LDPE, or to help develop C_{1s} component peak models, in the case of PP. Equation (2) was used to estimate the amount of organic oxide [%O (CO_x)], based on the relative areas of the O_{1s} and C_{1s} regions compared to the contribution of each CO_x environment from the high-resolution C_{1s} peak model.

$$\%O_{(CO_x)} = \frac{\frac{(C{-}O)+(C{=}O)+2(O{-}C{=}O)}{(C_{1s}\ \text{Total Area})+(C{-}O)+(C{-}O)+2(O{-}C{=}O)}}{\frac{\%O_{(O_{1s})}}{\%C_{(C_{1s})}+\%O_{(O_{1s})}}} \quad (2)$$

The %O (CO_x) is only an estimation because the ratio of carbon to oxygen in the alcohol/ether (C—O) binding environments depends on the relative contributions of the alcohol (C—O—H), ether (C—O—C), and ester (C—O—C═O) functional groups, as described in eq. (3).

$$\text{Area}_{(C-O)} = (\text{Alcohol}) + (\text{Ester}) + 0.5(\text{Ether}) \quad (3)$$

It is impossible to know, *a priori*, the precise distribution between functional groups in the alcohol-/ether-binding environment. We made the simplifying assumption that these functional groups exist primarily on the surface of the control and treated substrates; thus, the alcohol and acid would dominate relative to the ether and ester functional groups, thereby simplifying eq. (3) by assuming a carbon to oxygen ratio of 1 : 1.

RESULTS

Hydrophobic Recovery on Polyolefins

DSC was performed on untreated HDPE, LDPE, and PP to verify their thermal properties and to confirm their identity. In each case, the thermal properties are consistent with typical properties of these polymers.[39] The T_m of HDPE, LDPE, and PP are 140.5, 116.7, and 161.7°C, respectively. The T_g of PP, identified during the second heating cycle, occurs at −9.1°C. Careful inspection of the HDPE and LDPE traces does not reveal a measurable T_g, which typically occurs below −100°C for both examples of PE. Again, DSC was not attempted on H_2O plasma-treated polymer samples because the volume of the

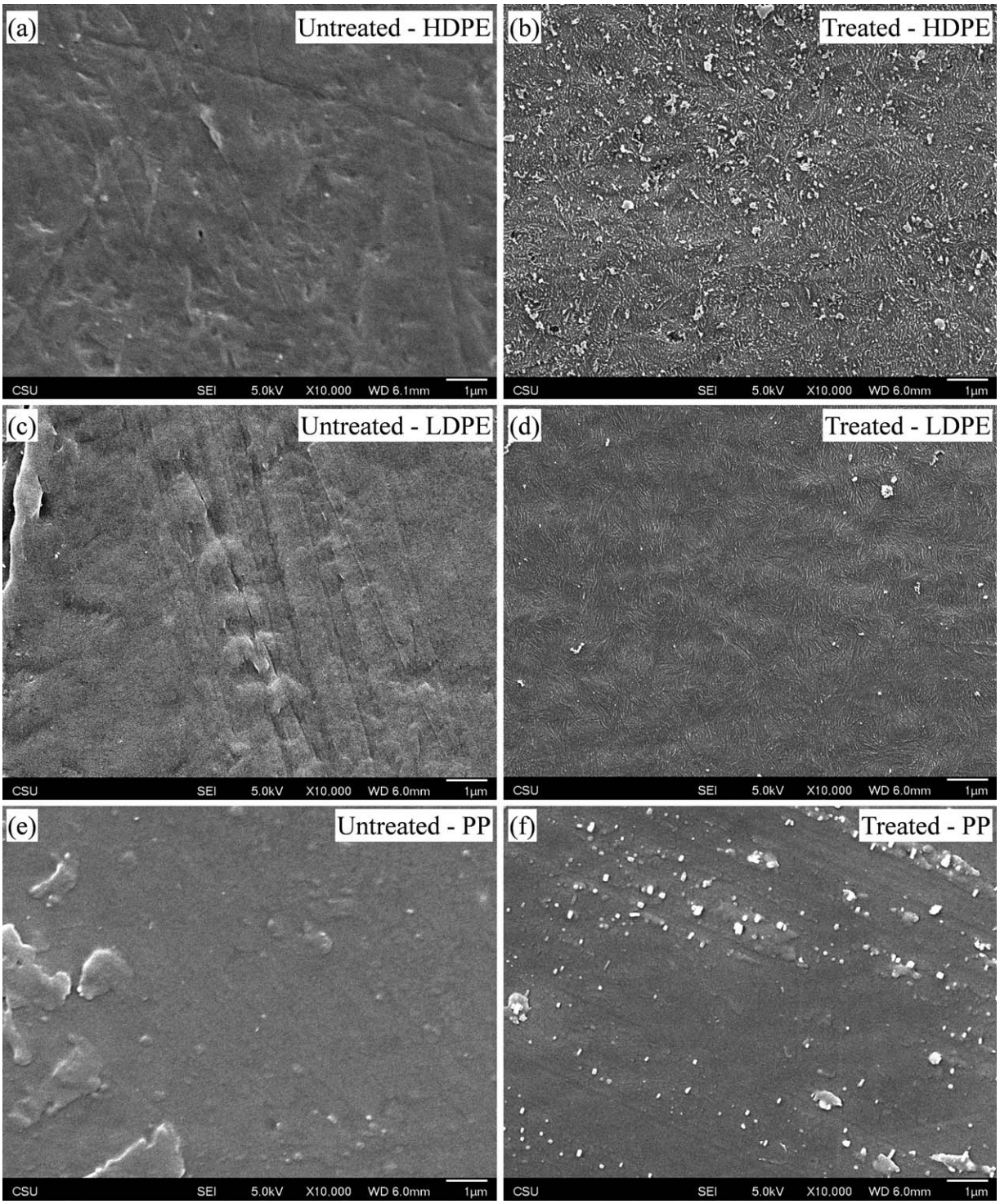

Figure 1. SEM images from untreated (left) and freshly treated (right) HDPE (a–b), LDPE (c–d), and PP (e–f).

modified surface layer is insignificant compared to the total volume of the bulk sample. Furthermore, modifying a subsample of a sufficiently small size for DSC would influence the results of the measurement compared to the larger sample sizes required for wCA or XPS measurements.

SEM imaging was performed to characterize any effect of H_2O plasma modification on surface morphology. Representative images from untreated and freshly treated HDPE, LDPE, and PP are shown in Figure 1. The surface of untreated HDPE and LDPE, Figure 1(a,c), consists of larger scale somewhat irregular features (scratches and striations), likely as a result of the manufacturing process and subsequent handling. The surface of H_2O plasma-treated HDPE and LDPE, by comparison, consists of a regular pattern of smaller scale roughness, Figure 1(b,d).

Table I. wCA and Elemental Composition of Untreated, Freshly Treated, and Aged H_2O Plasma-Modified HDPE, LDPE, and PP

Sample	Age	wCA (°)	Control wCA (°)	Elemental composition (%)[a]				
				Carbon	Oxygen	Silicon	O/C	Control O/C
Polyethylene	Untreated[b]			82.1 ± 3.2	10.9 ± 1.9	6.9 ± 1.3		
(High density)	Fresh	18 ± 3	101 ± 4	73.1 ± 0.1	23.2 ± 0.1	3.6 ± 0.1	0.318 ± 0.001	0.134 ± 0.028
	1 week	38 ± 4	102 ± 3	72.0 ± 0.7	23.6 ± 0.7	4.4 ± 0.2	0.328 ± 0.012	0.141 ± 0.012
	1 month	49 ± 4	102 ± 2	65.0 ± 3.4	27.9 ± 2.1	7.1 ± 1.3	0.431 ± 0.053	0.220 ± 0.054
Polyethylene	Untreated[b]			90.4 ± 0.9	5.7 ± 0.7	3.9 ± 0.3		
(Low density)	Fresh	50 ± 1	100 ± 1	82.8 ± 0.2	17.2 ± 0.2	-	0.207 ± 0.004	0.063 ± 0.008
	1 week	66 ± 1	102 ± 2	80.3 ± 0.6	17.7 ± 0.4	2.0 ± 0.2	0.221 ± 0.006	0.074 ± 0.010
	1 month	71 ± 1	99 ± 2	84.3 ± 0.1	15.7 ± 0.1	-	0.186 ± 0.001	0.053 ± 0.002
Polypropylene	Untreated[b,c]			85.7 ± 1.8	9.4 ± 1.1	2.7 ± 0.3		
	Fresh	71 ± 2	105 ± 2	79.0 ± 0.3	19.4 ± 0.1	1.7 ± 0.2	0.245 ± 0.002	0.110 ± 0.015
	1 week	89 ± 2	105 ± 1	80.8 ± 1.2	17.8 ± 1.3	1.4 ± 0.5	0.220 ± 0.018	0.088 ± 0.005
	1 month	108 ± 4	109 ± 3	86.0 ± 0.6	14.0 ± 0.6	-	0.163 ± 0.008	0.089 ± 0.010

[a] Reported error is one standard deviation.
[b] The reported untreated elemental composition is from the fresh cleaned control analysis, performed in conjunction with the freshly treated sample time point.
[c] Approximately, 2% nitrogen was also detected in this sample.

The scale of this roughness appears larger on HDPE compared to LDPE, and the large-scale features observed on the untreated samples are not as pronounced on either material. Similar changes in surface morphology appear to take place on PP with H_2O plasma modification, Figure 1(e,f).

The results from wCA measurements on HDPE, LDPE, and PP are listed in Table I. The wCAs measured on cleaned control samples are all $\geq 100°$, consistent with typical wCA measurements on polyolefin surfaces. H_2O plasma modification using standard treatment conditions results in a marked change in wettability on each polyolefin. For example, the wCA on HDPE decreases to $18 \pm 3°$ upon treatment, which amounts to a decrease in wCA of 82% compared to the fresh untreated control sample. Indeed, HDPE demonstrates the most significant change in wettability among purely aliphatic polymers. By comparison, the wCAs of LDPE and PP decrease by only 50 and 32%, respectively. Over the 1-month aging study, each polyolefin undergoes significant hydrophobic recovery, consistent with previous studies[34] on porous polymer membranes composed of similar materials. Here, we find that HDPE is the least susceptible to hydrophobic recovery. The wCA on HDPE samples aged for 1-month increase to $49 \pm 4°$, corresponding to a 36% recovery compared to freshly treated HDPE. By contrast, PP aged for month is indistinguishable from untreated control samples, exhibiting the greatest susceptibility to hydrophobic recovery.

The XPS elemental composition and calculated O/C results for HDPE, LDPE, and PP surfaces are listed in Table I. The O/C of cleaned control HDPE, LDPE, and PP surfaces each reveal the presence of significant oxygen. This could result from natural oxidation of the polymer surface or from adsorption of oxide-containing contaminates after cleaning. The presence of silicon on many of these samples suggests, however, that (1) silicone-based release agents were used during manufacturing and that these release agents persisted despite cleaning, or (2) silicon-containing additives are incorporated into the polymer and these additives were unaffected by cleaning. Upon treatment, the O/C increases for each polymer sample, consistent with the oxidizing nature of the H_2O plasma treatment and the observed decreases in wCA. Despite the hydrophobic recovery observed; however, XPS measurements do not reveal a corresponding pattern of decreasing O/C. Indeed, PP is the only material wherein the surface O/C on plasma treated samples evolves with age relative to the untreated control samples.

High-resolution C_{1s} spectra from untreated, freshly treated, and aged samples were further analyzed to ascertain the distribution of oxidized carbon (CO_x)-binding environments with H_2O plasma modification, Table II. For HDPE, the untreated sample comprises mostly C—C/C—H with trace amounts of the CO_x-binding environments, including C—O, C═O, and O—C═O functional groups. These CO_x-binding environments only account for $5.5 \pm 1.3\%$ of the total C_{1s} peak area, meaning that the %O (CO_x) only accounts for $47 \pm 6\%$ of the total oxygen concentration on the sample surface, based on eq. (2). This result suggests that the oxygen indeed originates from the three possible sources of contamination noted previously: oxidation of the polymer surface, adsorption of oxidized carbon contaminants, and persistent silicone-based release agents. Upon treatment, the area of each CO_x-binding environment increases, consistent with oxidation of the polymer surface during treatment. Considering a similar analysis of the oxygen-binding environment distributions for the treated sample, the CO_x environments account for $22 \pm 0.3\%$ of the total C_{1s} peak area on the freshly treated HDPE sample, corresponding to $91 \pm 1\%$ of the oxygen concentration on the sample surface. The high-resolution C_{1s} fitting results from the 1 week and 1 month aged HDPE samples suggest that these CO_x binding environments

Table II. C_{1s} Moiety Distribution of Untreated, Freshly Treated, and Aged H_2O Plasma-Modified HDPE, LDPE, and PP

		C_{1s} relative contribution (%)[a]			
Sample	Age	Aliphatic	C—O	C=O	O—C=O
Polyethylene	Untreated[b]	94.5 ± 1.3	3.1 ± 0.8	1.9 ± 0.5	0.4 ± 0.1[c]
(High density)	Fresh	78.1 ± 0.3	11.4 ± 0.5	4.3 ± 0.3	6.2 ± 0.2
	1 week	80.1 ± 2.6	10.1 ± 1.4	5.0 ± 0.4	4.8 ± 1.2
	1 month	77.8 ± 0.3	11.6 ± 0.1	5.2 ± 0.3	5.5 ± 0.1
Polyethylene	Untreated[b]	97.8 ± 0.8	1.8 ± 0.4	0.4 ± 0.4	-
(Low density)	Fresh	80.0 ± 0.6	10.5 ± 0.6	4.1 ± 0.1	5.3 ± 0.1
	1 week	81.6 ± 0.3	9.2 ± 0.5	5.4 ± 0.6	3.9 ± 0.2
	1 month	82.3 ± 0.3	8.3 ± 0.1	5.4 ± 0.1	4.0 ± 0.3
Polypropylene	Untreated[b]	91.4 ± 2.2	4.8 ± 1.6	3.4 ± 0.6	0.5 ± 0.1
	Fresh	79.2 ± 1.2	11.1 ± 1.2	4.9 ± 0.4	4.9 ± 0.4
	1 week	80.7 ± 0.3	11.0 ± 0.6	3.1 ± 0.7	5.2 ± 0.4
	1 month	85.0 ± 0.3	9.3 ± 0.2	1.0 ± 0.3	4.7 ± 0.2

[a] Reported error is one standard deviation.
[b] The reported untreated sample is the fresh cleaned control analysis, performed in conjunction with the freshly treated sample time point.
[c] Reported error is three standard deviations.

are stable, Table II. However, CO_x only accounts for 80 ± 8 and 72 ± 6% of the total oxygen on the 1 week and 1 month HDPE samples, respectively. These decreases in surface CO_x coincide with an increase in the surface silicon concentration and suggest that the surface is unstable. As the greatest change in surface composition is most pronounced between the fresh and one week time points, this may contribute to the measureable hydrophobic recovery observed over this period. Representative HDPE high-resolution C_{1s} XPS spectra from each aging time point can be found in Supporting Information (Figure S1).

Spectra of cleaned control and freshly treated LDPE samples reveal similar changes following H_2O plasma modification. Representative spectra are shown in Figure 4 and results from their deconstruction are listed in Table II. The distribution of CO_x-binding environments is similar to that on HDPE. The lower oxygen concentration on LDPE is reflected in the magnitude of the CO_x-binding environments, where %O (CO_x) represents only 35 ± 10% of the total oxygen concentration on the sample surface. Surface modification of LDPE leads to a similar distribution of CO_x-binding environments compared to HDPE. On freshly treated LDPE %O (CO_x) accounts for 117 ± 2% of the oxygen concentration on the sample surface. This high percentage is consistent with the absence of silicon in these samples. The fitting results from high-resolution C_{1s} XPS analysis of plasma-treated LDPE samples aged for 1 week and 1 month do not change appreciably and the CO_x-binding environments continue to represent the majority of the oxygen detected on the sample surface. Representative LDPE high-resolution C_{1s} XPS spectra from each aging time point can be found in the Supporting Information (Figure S2).

Spectra from PP samples were fit using a slightly different procedure compared to the other polyolefins. Initial attempts to fit the PP samples revealed that changes in the CO_x peak areas were inconsistent as the samples aged. As this was likely an artifact resulting from the CO_x components shifting to lower BEs as the samples aged, we developed a procedure by which we used %O (CO_x) to substantiate the BE shift of each CO_x component. The %O (CO_x) represented 104 ± 5% of the total oxygen on the freshly treated PP sample. Assuming that oxygen loss pathways were unlikely to involve conversion to some

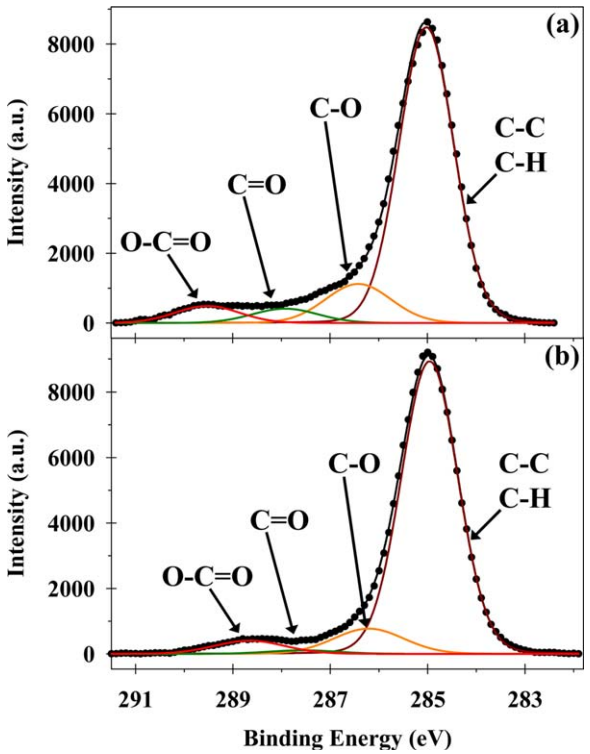

Figure 2. High-resolution C_{1s} XPS spectra from (a) freshly treated PP and (b) treated PP aged for 1 month. [Color figure can be viewed in the online issue, which is available at wileyonlinelibrary.com.]

Table III. C_{1s} Moiety-Binding Energies of Freshly Treated and Aged H_2O Plasma-Modified PP

Age	Fitting error (mean χ^2)[a]	Polypropylene C_{1s} moiety-binding energy (eV)			
		Aliphatic	C—O	C=O	O—C=O
Fresh	2.2583 ± 0.5899	285.00	286.40	287.90	289.50
1 week	0.8034 ± 0.5321	285.00	286.30	287.70	289.20
1 month	1.3716 ± 0.3563	285.00	286.25	287.60	288.70

[a] Reported error is one standard deviation.

persistent inorganic oxide, the proportion of oxygen represented by CO_x in the C_{1s} spectrum should remain constant. This assumption is supported by the silicon concentration measured on the treated PP sample surface, which is slightly above the limit of detection and disappears completely as the PP ages. The result of this fitting technique shows that despite shifts in CO_x BE over one month, Figure 2, the areas of the CO_x peaks evolved in a fashion similar to HDPE and LDPE, Table II, while yielding favorable χ^2 values, Table III. Cleaned control PP is very similar to HDPE and LDPE, consisting primarily of C—C/Cdbond]H with small amounts of C—O, C=O, and O—C=O functionalities, Table II. H_2O plasma treatment also resulted in similar increases in each of the CO_x-binding environments, Figure 3a, and their contributions stay relatively constant during aging, Figure 3b. Representative PP high-resolution C_{1s} XPS spectra from each aging time point can be found in the Supporting Information (Figure S3).

The shift in CO_x BEs is an interesting phenomenon, Table III and provides insight into processes occurring at the surface of PP during aging. The BEs of each CO_x moiety on freshly treated PP are identical to those of HDPE and LDPE. As the PP surface ages, however, these BEs shift to lower energy. The magnitude of a given shift appears to coincide with the degree of oxidation of that CO_x moiety. For example, the BE of the O—C=O group after one month is 0.8 eV lower when compared to the freshly

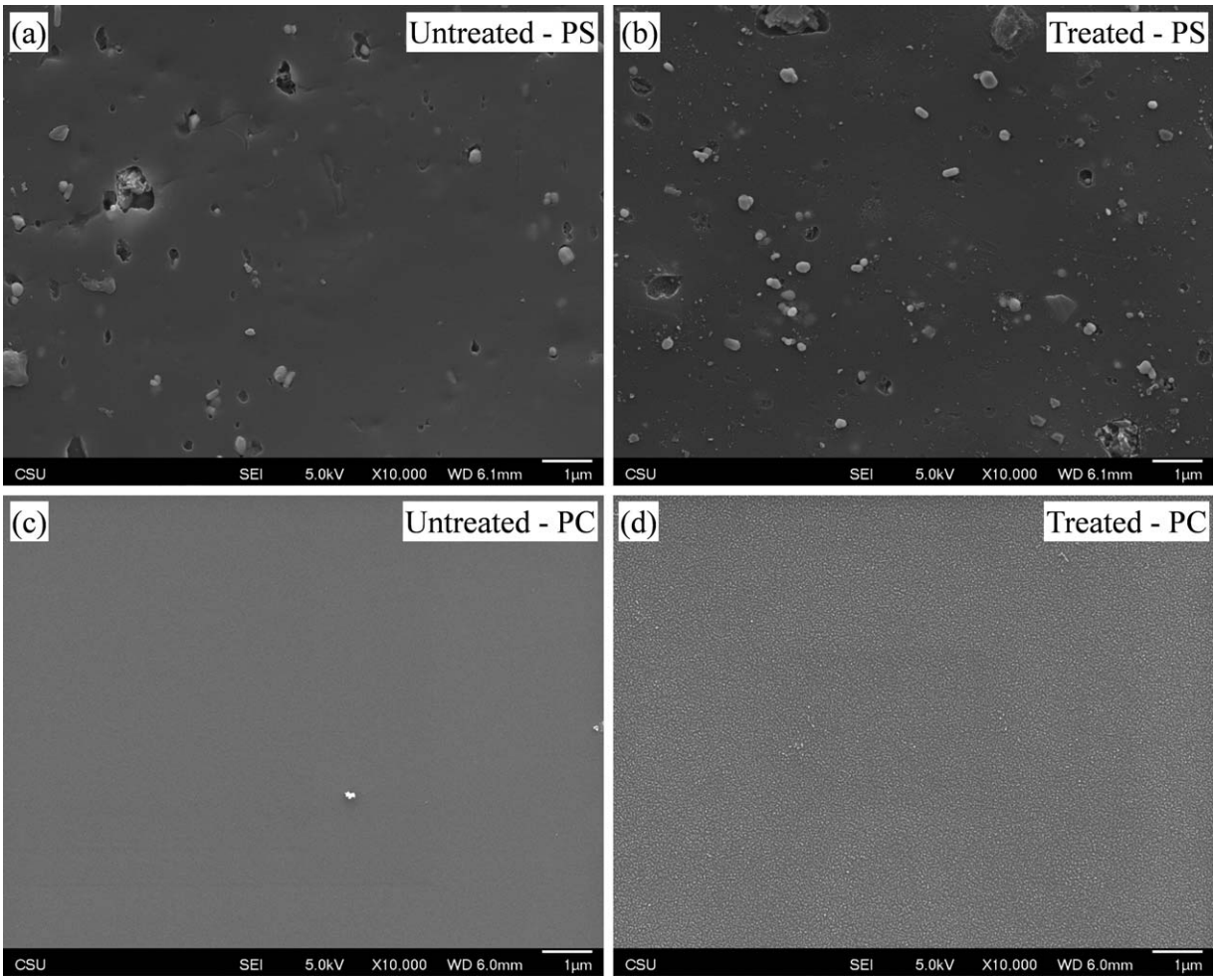

Figure 3. SEM images from untreated (left) and freshly treated (right) PS (a–b) and PC (c–d).

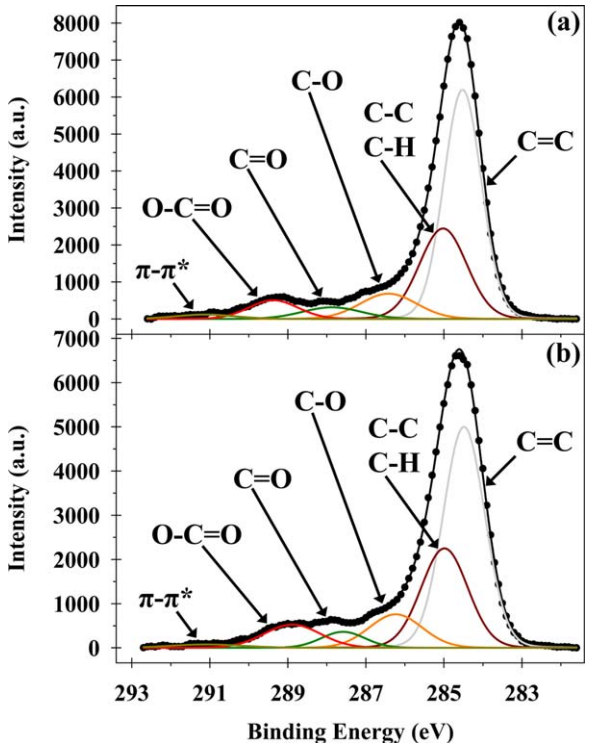

Figure 4. High-resolution C_{1s} XPS spectra from (a) freshly treated PS and (b) treated PS aged for 1 month. [Color figure can be viewed in the online issue, which is available at wileyonlinelibrary.com.]

treated PP sample. Shifts in BE such as these result from changes in the local chemical environment of a functional group[40] and are discussed further below.

Hydrophobic Recovery on Aromatic Polymers

DSC was performed on untreated PS and PC to verify their thermal properties. Again, the thermal properties are consistent with typical properties of these polymers.[39] The T_g of PS and PC were found to be 102.3 and 150.9°C, respectively. The T_m of PC was found to be 153.6°C with an additional melting feature found at 203.6°C, which was only present during the first heating cycle only. Given that thermal decomposition typically accompanies melting of PS, no attempt was made to heat untreated PS beyond 250°C. As mentioned previously, DSC was not attempted on H_2O plasma-treated polymer samples because the volume of the modified surface layer is insignificant compared to the total volume of the bulk sample.

Representative SEM images from untreated and freshly treated PS and PC are shown in Figure 3. Untreated PS is generally flat with small surface structures and inclusions visible at the surface, Figure 3a. There are no visible changes to the freshly H_2O plasma-treated PS surface, Figure 3b. At the scale of the SEM performed here, untreated PC has no visible features (Figure 4c). H_2O plasma-treated PC, however, has a visible regular surface roughness consisting of small nodules (Figure 4d). These changes in surface morphology on PC have been noted in previous studies[37] and are believed to be the result of redeposition of reduced carbon or differential etching associated with reduced carbon deposits that coincide with the presence of hydrogen in the H_2O plasma system.

Results from wCA measurements on PS and PC are listed in Table IV. The wCAs measured on cleaned control PS and PC are $93 \pm 4°$ and $88 \pm 4°$, respectively. The increased variance in these measurements results from more diverse functionality in these polymers, compared to the polyolefin series. H_2O plasma modification using standard treatment conditions results in a marked change in wettability for both polymer materials. Coincidentally, the wCA measurements on PS and PC are the same within error ($21 \pm 4°$ and $25 \pm 2°$, respectively). During aging, both polymers undergo significant hydrophobic recovery, consistent with previous studies of PS and PC modification.[25,35,41–45] Here, we find that PC is the least susceptible to hydrophobic recovery, yielding similar performance to HDPE. The wCA on PC samples aged for 1 month increases to $47 \pm 1°$, corresponding to a 34% recovery compared to freshly treated PC. By contrast, PS is far more susceptible to hydrophobic recovery. After 1 month of aging, the wCA begins to approach that measured on untreated control samples, corresponding to a 69% recovery compared to the untreated sample.

Table IV. wCA and Elemental Composition of Untreated, Freshly Treated, and Aged H_2O Plasma-Modified PS and PC

Sample	Age	wCA (°)	Control wCA (°)	Elemental composition (%)[a]				
				Carbon	Oxygen	Silicon	O/C	Control O/C
Polystyrene	Untreated[b,c]			81.4 ± 3.2	12.2 ± 2.1	4.4 ± 0.3		
	Fresh	21 ± 4	93 ± 4	79.0 ± 2.2	21.0 ± 2.2	-	0.267 ± 0.035	0.151 ± 0.032
	1 week	53 ± 2	94 ± 2	79.6 ± 0.4	20.4 ± 0.4	-	0.257 ± 0.007	0.096 ± 0.009
	1 month	70 ± 1	83 ± 9	77.5 ± 1.4	21.7 ± 1.1	-	0.280 ± 0.020	0.138 ± 0.004
Polycarbonate	Untreated[b]			84.3 ± 0.2	15.7 ± 0.2	-		
	Fresh	25 ± 2	88 ± 4	74.6 ± 0.3	25.4 ± 0.3	-	0.341 ± 0.005	0.187 ± 0.003
	1 week	41 ± 1	91 ± 1	73.7 ± 0.1	26.3 ± 0.1	-	0.357 ± 0.001	0.188 ± 0.002
	1 month	47 ± 1	89 ± 3	75.3 ± 0.2	24.7 ± 0.2	-	0.329 ± 0.003	0.195 ± 0.007

[a] Reported error is one standard deviation.
[b] The reported untreated elemental composition is from the fresh cleaned control analysis, performed in conjunction with the freshly treated sample time point.
[c] Approximately 2% nitrogen was also detected in this sample.

Table V. C_{1s} Moiety-Binding Energies of Freshly Treated and Aged H_2O Plasma-Modified PS

Age	Fitting error (mean χ^2)[a]	Polystyrene C_{1s} moiety-binding energy (eV)				
		Aromatic	Aliphatic	C—O	C=O	O—C=O
Fresh	1.0234 ± 0.3497	284.50	285.00	286.40	287.85	289.35
1 week	1.3770 ± 0.2080	284.50	285.00	286.30	287.65	289.05
1 month	1.4732 ± 0.3913	284.50	285.00	286.25	287.60	288.90

[a] Reported error is one standard deviation.

XPS was used to measure the elemental composition of PS and PC surfaces (Table IV). The O/C of the cleaned control PS and PC surfaces each reveal the presence of significant oxygen. PC contains native oxygen functionality and the sources of oxygen on untreated PS are likely the same as those discussed above for the untreated polyolefin polymers. Upon treatment, the O/C increases for both polymer samples, consistent with the oxidizing nature of the H_2O plasma treatment and the observed decreases in wCA. Despite the hydrophobic recovery observed on both polymers, however, XPS measurements do not reveal a corresponding pattern of decreasing O/C.

High-resolution C_{1s} XPS spectra from untreated, freshly treated, and aged PS samples were fit using a similar procedure to that used for PP but with a slightly different set of binding environments. The reduced carbon was fit assuming contributions from aliphatic carbon (C—C/C—H, 285.0 eV) and allylic carbon (C=C/C=C—H, 284.5 eV) to account for the presence of aromatic functionality on the polymer backbone. The BE of the C=C/C=C—H-binding environment was not constrained. Similar to PP, initial attempts to fit the PS sample spectra revealed that the peak areas were changing erratically as the samples aged. In this case, the ratio of C—C/C—H and C=C/C=C—H peak areas appeared to be changing. It is unlikely that stable aromatic functionality would continue to spontaneously convert to aliphatic functionality to the extent suggested by this change. Again this was compensated for in the modeling by allowing the CO_x components to shift to progressively lower BEs for aged samples (Figure 3). Unlike in our analysis of PP, however, the positions of the CO_x-binding environments were adjusted to optimize the shape of the C_{1s} region where the C—C/C—H and C=C/Cdbond]C—H-binding environments are located. The resulting PS fitting χ^2 values are generally favorable and are listed in Table V.

Results from fitting the PS C_{1s} spectra are listed in Table VI. Untreated PS comprises primarily C=C/C=C—H and C—C/C—H functionalities. From this measurement, the aromatic/aliphatic ratio is 4.6, somewhat higher than the expected ratio of 3. When the CO_x peak area is added to the aliphatic component in this calculations the ratio decreases to 3.6. This would suggest that the native surface oxidation exists on the aliphatic backbone of PS, consistent with the stability of aromatic functionality that comprises the rest of the polymer. The area of each CO_x-binding environment increases upon plasma treatment (Figure 5a) and continues to increase slightly as the samples age (Figure 5b). This is largely at the expense of the C=C/C=C—H-binding environment, suggesting that the aromatic functionality affected by plasma treatment continues to oxidize as the surface ages. Moreover, each CO_x-binding environment shifts to lower BE as the surface ages (Table V). Notably, these shifts are very similar to those observed on aged PP surfaces, the only other polymer found to undergo significant hydrophobic recovery. Representative PS high-resolution C_{1s} XPS spectra from each aging time point can be found in the Supporting Information (Figure S4).

Spectra from untreated and freshly treated PC samples were fit using a similar procedure to that used for PS, with some

Table VI. C_{1s} Moiety Distribution of Untreated, Freshly Treated, and Aged H_2O Plasma-Modified PS and PC

Sample	Age	C_{1s} relative contribution (%)[a]					
		Aromatic	Aliphatic	C—O	C=O	O—C=O	O=C(—O)$_2$
Polystyrene[c]	Untreated[b]	78.1 ± 5.4	17.1 ± 3.4	3.1 ± 1.0	1.5 ± 0.8	0.2 ± 0.2	-
	Fresh	54.5 ± 0.5	27.4 ± 0.5	9.3 ± 0.3	3.4 ± 0.8	5.4 ± 0.5	-
	1 week	53.6 ± 0.5	27.0 ± 0.3	11.0 ± 0.7	2.3 ± 0.2	6.3 ± 0.2	-
	1 month	52.1 ± 0.2	26.2 ± 0.1	11.3 ± 1.1	3.2 ± 0.8	7.2 ± 0.2	-
Polycarbonate[c]	Untreated[b]	80.3 ± 0.1[d]		13.8 ± 0.4	-	-	5.9 ± 0.3
	Fresh	65.2 ± 1.1[d]		21.5 ± 1.1	3.6 ± 0.7	4.8 ± 0.4	4.9 ± 0.1
	1 week	66.5 ± 0.7[d]		20.9 ± 0.5	4.1 ± 0.8	3.7 ± 0.3	4.8 ± 0.1
	1 month	67.1 ± 0.6[d]		21.0 ± 0.7	3.5 ± 0.2	3.6 ± 0.5	4.7 ± 0.5

[a] Reported error is one standard deviation.
[b] The reported untreated sample is the fresh control analysis, performed in conjunction with the freshly treated sample time point.
[c] Samples had significant contributions from π–π^* transition. This area was ignored for relative contribution calculations.
[d] Aliphatic and aromatic C—C/C—H regions were fit as one peak to improve fitting reproducibility and minimize error.

exceptions. Despite the presence of aromatic functionality in bisphenol A-based PC, the carbon peak was fit with one component representing both allylic and aliphatic carbon functionalities. Spectra from H_2O plasma-treated PC were fit using only a Shirley baseline to be as consistent as possible because there was no practical method for determining the appropriate linear contribution for a mixed baseline. The results from PC deconvolution are listed in Table VI. Untreated PC is composed of C—C/C—H/C=C, C—O, and O=C(—O)$_2$ functionalities in proportions consistent with bisphenol A PC, similar to that reported previously.[14] Following plasma treatment, the surface of the freshly treated sample is generally more oxidized, resulting in significantly more C—O along with the introduction of C=O and O—C=O functional groups. This oxidation occurs at the expense of the C—C/C—H/C=C and O=C(—O)$_2$-binding environments, consistent with other reports.[46] Samples aged for 1 month show very little change in the distribution of CO_x-binding environments, and there are no BE shifts observed. Representative PC high-resolution C_{1s} XPS spectra from each aging time point can be found in Supporting Information (Figure S5).

DISCUSSION

In our group, previous studies examined aging effects on polymeric membranes, including PSf, PES, and PE, following treatment using H_2O vapor plasma.[34] From the previous studies, it was demonstrated that some membranes exhibited hydrophobic recovery (e.g., PE) and others did not (e.g., PSf and PES). This study seeks to further investigate these phenomena by undertaking a more comprehensive study of H_2O plasma treatments on different classes of polymer materials, namely polyolefins and polymers with aromatic functionality.

Increased Wettability and Hydrophobic Recovery on Polyolefins

Each polyolefin responds to H_2O plasma treatment in the same way. The otherwise hydrophobic polyolefin surface is rendered more wettable via the implantation of new polar surface functionalities. Here, we find that initial improvement in wettability from highest to lowest is HDPE > LDPE > PP. Changes in wettability can result from either changes in surface functionality or surface morphology. Changes in elemental composition measured using XPS show the incorporation of new oxygen functionalities on each material following plasma modification. We also note increases in surface roughness on each material. While increased surface roughness likely contributes to the measured change in wCA, it alone cannot explain the observed decrease in wCA on each polymer. Increased roughness on a hydrophobic material causes the observed wCA to increase. We conclude, therefore, that implantation of new polar functionality is primarily responsible for the observed change. This distinction is important because any proposed hydrophobic recovery mechanism must address the ultimate fate of these oxidized moieties. We find that the extent of hydrophobic recovery from highest to lowest recovery is PP > LDPE > HDPE. In each case, the loss of oxygen on the surface cannot fully describe the observed recovery behavior.

One possible hypothesis to explain hydrophobic recovery on polyolefins is that the thermal properties dictate surface reorganization. If the amount of energy required to reorganize the polymer chains was sufficiently small, the rate and extent to which polar surface functionalities are subsumed would increase. Under those circumstances, low T_m and T_g at the polymer surface would correlate with the tendency of a surface to undergo hydrophobic recovery. This simple relationship, however, does not account for the observation that PP has the highest T_m and T_g and is simultaneously the most prone to hydrophobic recovery.

Treated PE is very wettable and exhibits little hydrophobic recovery, whereas treated PP is less wettable and exhibits complete hydrophobic recovery. These observations suggest that these polymer surfaces respond to plasma modification differently. A similar trend was observed by Jokinen *et al.*,[35] who showed that PP is more susceptible to hydrophobic recovery after O_2 plasma modification and attributed it to the formation of LMWOM during plasma treatment that subsequently reorganizes with aging. Likewise, Guimond and Wertheimer[47] used air and N_2 atmospheric pressure glow discharges to modify the surface of LDPE and PP and also observed significant formation of LMWOM on PP. Again, LMWOM formation correlated with the extent of hydrophobic recovery during aging. Behnisch *et al.*[48] compared oxygen plasma treatments on PE and PP surfaces and found that ultrasonic cleaning immediately after plasma treatment produced a much higher wCA on PP. They cited the work of Garbassi and coworkers,[49] explaining that PP is prone to chain scission during plasma treatment, whereas PE is more likely to crosslink. From these literature accounts, the reason why PP is more susceptible to reorganization following H_2O plasma modification is similar to the thermal properties hypothesis discussed earlier. Chain scission alters the thermal properties of a very thin surface layer on PP, thereby lowering the energy barrier for reorganization. Polar functionalities are buried and a nonpolar surface is presented, decreasing surface energy and wettability. Cross-linking on PE, however, prevents hydrophobic recovery by creating an interconnected network of polymer chains on the surface. This anchors polar functionalities at or near the surface and increases the energy required to reorganize the polymer.

The observation that O/C remains unchanged after the surface reorganizes can be explained by noting that the diffusion distance of LMWOM fragments is less than the sampling depth of the XPS measurement. This is corroborated by the work of Truica-Marasescu *et al.*,[17] who used time of flight-secondary ion mass spectrometry to examine LDPE and PP surfaces modified in NH_3 using VUV light and noted that polar groups migrated below the surface but remained within the sampling depth of XPS (~10 nm). Although elemental composition data cannot be used to follow surface reorganization, high-resolution XPS peak fitting does give us insight into this process. Work described previously[40] correlates shifts in C_{1s} CF_x BEs with changes in the local chemical environment. As the local concentration of fluorine decreased, the BEs of individual moieties decreased because of the lower electron withdrawing power on the carbon center. A similar analysis of C_{1s} CO_x BEs was

conducted on treated and aged polymers in this study. XPS spectra reveal significant shifts in CO_x BEs as the PP surface ages, whereas the BEs of CO_x moieties on HDPE and LDPE surfaces remain constant over the same period. As polar functionalities are subsumed by the PP surface, the oxygen atoms are further influenced by nearby carbon atoms. The additional electron density from these interactions decreases the withdrawing power of the oxygen and, concomitantly, decreases the C_{1s} BE of the CO_x functional group.

Comparing HDPE and LDPE, wCA results show H_2O plasma treatments are more effective at creating hydrophilic surfaces with HDPE samples. Silicon residues, detected before and after treatment, may be contributing to this improved performance as they can be converted to either an intermediate oxidation state of silicon (Si_xO_y) or to SiO_2 during treatment.[50] H_2O plasma treatments of silicon wafers showed those surfaces are populated with SiOH functional groups, yielding low wCAs.[50] Although some of the silicon on our polymer surfaces is lost during H_2O plasma treatment, the silicon that remains is likely oxidized to SiO_2 which contributes to the low wCA we observe on freshly treated HDPE. Regardless, calculations reveal a persistent increase in CO_x relative to inorganic carbon. Given that no changes in CO_x BE, associated with long-range rearrangements, were observed, CO_x functionalities remain at the surface and continue to contribute to improved wettability as both PE materials age.

The extent of HDPE and LDPE hydrophobic recovery suggests the HDPE surface is more stable. This is surprising as XPS measurements reveal changes in oxygen and silicon distribution with treatment and aging on HDPE. A significant portion of the oxygen on untreated HDPE exists in the form of inorganic oxide likely bound to the silicon contamination. The H_2O plasma removes a significant amount of this silicon, leaving the majority of the oxygen in the form of CO_x. As the treated samples age, the distribution of organic oxide to inorganic oxide reverts coinciding with the amount of silicon measured by XPS. These results suggest that the silicon contamination was not just on the surface of the HDPE and is likely diffusing from the bulk of the HDPE sample. Although a possible source of silicon is silicone oils applied as release agents during HDPE manufacturing, these would be expected to exacerbate hydrophobic recovery. Additional experiments are required to discover the identity of these contaminates, compare different sources of silicon contamination, and learn their impact on polyolefin surface aging.

Hydrophobic Recovery on Polystyrene

PS is far more wettable following H_2O plasma modification and exhibits significant aging behavior, resulting in the second highest hydrophobic recovery of the materials included in this study. Again, the thermal properties of PS cannot be used to explain the extent of hydrophobic recovery. In this case, even more so, as the T_g and decomposition temperatures of PS are significantly higher than ambient temperature and far beyond those of HDPE and LDPE. Morphology also does not play a role in improved wettability or subsequent hydrophobic recovery, as no change in surface morphology was observed with treatment.

To our knowledge, there are no published accounts of $H_2O_{(g)}$ plasma modifications on PS. Garbassi and coworkers[25,44] examined the aging of PS after O_2 plasma surface modification. They found that all samples were subject to significant hydrophobic recovery, regardless of *P*, polymer molecular weight (MW), or storage temperature. They demonstrated that increased storage temperature during aging exacerbates hydrophobic recovery and that low M_W PS is more susceptible to hydrophobic recovery.[25] They attributed this to short- and long-range rearrangements driven by surface thermodynamics. From this, it would seem reasonable to assume that increasing the energy required to rearrange the polymer structure would reduce the extent of hydrophobic recovery. Larrieu, *et al.*[42] compared O_2 plasma modification of atactic (less crystalline) and isotactic (more crystalline) polystyrene, however, finding that both were equally susceptible to hydrophobic recovery immediately after treatment.

The notable hydrophobic recovery on PP has been attributed to surface rearrangement exacerbated by chain scission, and presumably, the same mechanisms are responsible for aging effects on the PS surface. Garbassi and coworkers[25] quantified surface cross-linking by gravimetric analysis of the insoluble fraction of plasma-treated PS and showed that low *P* does not induce cross-linking and leads to increased hydrophobic recovery. This is especially true for low M_W PS, ostensibly because it is the most susceptible to diffusion-based hydrophobic recovery. Although gravimetric analysis experiments revealed that high *P* could induce cross-linking on the PS surface, interestingly, this did not prevent hydrophobic recovery even at decreased storage temperatures. Thus, short-range rearrangement of implanted polar functional groups is likely responsible for inducing hydrophobic recovery, regardless of cross-linking or storage temperature. This is further supported by the work of two other studies. Murakami *et al.*[45] found that PS samples cross-linked prior to O_2 plasma treatment were susceptible to additional hydrophobic recovery even when attempts were made to remove the LMWOM thought to contribute to diffusion-based rearrangements. It was only when samples were stored in H_2O that hydrophobic recovery was prevented. Larsson and Derand[43] found that high *P* (500 W) O_2 plasma and a correspondingly high self-bias voltage (600 V) somewhat reduced hydrophobic recovery, although the induced surface roughness accompanying the higher *P* treatment may also be contributing.

Hydrophobic Recovery on Polycarbonate

The results of H_2O plasma modification and subsequent aging behavior of solid bisphenol A PC (Lexan®) is similar to that of track-etched PC membranes. PC membranes were rendered wettable by the H_2O plasma modification and this effect generally persists, showing only a small, but manageable amount of hydrophobic recovery.[14] An expanded study[37] looked more broadly at the mechanism of PC surface modification and etching from exposure to oxidizing plasma conditions, finding that oxygen and, to a lesser extent, hydroxyl radicals are primarily responsible for etching the PC surface. Interestingly, SEM images obtained in that study are consistent with those presented here. This provides further evidence that hydrogen-containing plasma systems cause a noticeable surface texture to

form on PC. While further studies are required to identify the nature of these features, they do not appear to hinder wettability or stability of modified PC. The remainder of this discussion will be limited to H_2O plasma modification of PC in comparison to the other polymer materials.

The properties and structure of PC are very different from those of polyolefins. Like PP and PS, plasma modification of PC is believed to result in a significant amount of chain scission and comparatively little cross-linking. Hofrichter *et al.*[51] compared O_2 plasma treatments on high-purity spin-coated PC substrates and commercially available Lexan®. They found their treatments induced chain scission on spin coated PC and that impurities in the surface of their Lexan® samples facilitated cross-linking. Muir *et al.*[52] examined O_2 plasma modification on optical grade Lexan® and noted formation of LMWOM, even with short treatment times (> 10 s). They attribute this to chain scission at the aromatic and carbonate groups in the PC backbone. The LMWOM formed as a result of chain scission was easily washed away, confirming its role in the stability of modified PC surfaces.

In light of the tendency for PC surfaces to undergo chain scission, the unique stability of PC requires another explanation. The wettability and aging performance of PC are comparable to polymers such as PSf and PES, studied previously.[13,33,34] These thermally stable polymers contain aromatic functionality within their polymer backbone and have been shown to have a similar response to oxidizing plasma conditions. Gonzalez *et al.*[53] showed O_2 plasma treatments cause aromatic ring opening in PSf and PES materials, which, taken to its fullest extent, would lead to chain scission; it is unclear from the literature, however, if cross-linking confers additional stability to PSf and PES. Although it would be reasonable to assume that the thermal stability assists in preventing aging effects and hydrophobic recovery PSf, PES, and PC, the fact that unmodified PS enjoys some degree of thermal stability and still demonstrates significant hydrophobic recovery suggests that another explanation is needed. It may be that a combination of factors such as crystallinity, π–π interactions, and thermal stability act together to stabilize to the modified surfaces. Regardless, H_2O plasma-modified PC materials have excellent wettability and hydrophobic recovery performance in the context of this study.

SUMMARY

The research described herein furthers our understanding of H_2O plasma modifications on several polymer surfaces. The H_2O plasma-modified polymers included in this study exhibit similar hydrophobic recovery behavior to polymers modified using other common oxidizing plasma systems (e.g., O_2) described in literature. This suggests that the hydrophobic recovery performance following oxidation and functional group implantation is intrinsic to the polymer. Each treated polyolefin sample is rendered wettable from the implantation of CO_x functional groups and exhibits some degree of hydrophobic recovery when aged. The treated HDPE surface is the most stable owing to plasma-induced cross-linking, whereas the treated PP surface is the least stable as a result of chain scission leading to significant surface rearrangement. H_2O plasma modification outcomes on the two polymers containing aromatic functionality differ dramatically from each other. Modified PC surfaces are rendered wettable and show excellent stability with age. Although chain scission is the dominant process on PC, some combination of factors, including thermal stability, limits hydrophobic recovery. PS is initially rendered wettable, but the aged PS samples exhibit behavior similar to that of PP. Shifts in the XPS C_{1s} CO_x moiety BEs of both PS and PP are consistent with polar functionalities being subsumed by the polymer surface as samples age. These results validate that H_2O plasma modifications are broadly applicable and give improved wettability to a range of polymers.

ACKNOWLEDGMENTS

Funding was provided by the National Science Foundation (CHE-1152963).

REFERENCES

1. Hall, C.; Murphy, P.; Griesser, H. *Plasma Processes Polym.* **2012**, *9*, 855.
2. Hall, C. J.; Murphy, P. J.; Griesser, H. J. *ACS Appl. Mater. Interfaces* **2014**, *6*, 1279.
3. Intranuovo, F.; Howard, D.; White, L. J.; Johal, R. K.; Ghaemmaghami, A. M.; Favia, P.; Howdle, S. M.; Shakesheff, K. M.; Alexander, M. R. *Acta Biomater.* **2011**, *7*, 3336.
4. De Bartolo, L.; Morelli, S.; Bader, A.; Drioli, E. *Biomaterials* **2002**, *23*, 2485.
5. Howarter, J. A.; Youngblood, J. P. *J. Colloid Interface Sci.* **2009**, *329*, 127.
6. Baytekin, H. T.; Wirth, T.; Gross, T.; Treu, D.; Sahre, M.; Theisen, J.; Schmidt, M.; Unger, W. E. S. *Surf. Interface Anal.* **2008**, *40*, 358.
7. Gururaj, T.; Subasri, R.; Raju, K. R. C. S.; Padmanabham, G.; Raju, K. *Appl. Surf. Sci.* **2011**, *257*, 4360.
8. Hofrichter, A.; Bulkin, P.; Drevillon, B. *J. Adhes. Sci. Technol.* **2002**, *16*, 395.
9. Muir, B.; Thissen, H.; Simon, G.; Murphy, P.; Griesser, H. *Thin Solid Films* **2006**, *500*, 34.
10. Xu, W. D.; Chellam, S. *Environ. Sci. Technol.* **2005**, *39*, 6470.
11. Zhang, M. M.; Li, C.; Benjamin, M. M.; Chang, Y. J. *Environ. Sci. Technol.* **2003**, *37*, 1663.
12. Qu, F.; Liang, H.; Zhou, J.; Nan, J.; Shao, S.; Zhang, J.; Li, G. *J. Membr. Sci.* **2014**, *449*, 58.
13. Kull, K. R.; Steen, M. L.; Fisher, E. R. *J. Membr. Sci.* **2005**, *246*, 203.
14. Tompkins, B. D.; Dennison, J. M.; Fisher, E. R. *J. Membr. Sci.* **2013**, *428*, 576.
15. Shi, X.; Field, R.; Hankins, N. *Desalin. Water Treat.* **2011**, *35*, 68.
16. O'Connell, C.; Sherlock, R.; Ball, M. D.; Aszalós-Kiss, B.; Prendergast, U.; Glynn, T. J. *Appl. Surf. Sci.* **2009**, *255*, 4405.

17. Truica-Marasescu, F.; Jedrzejowski, P.; Wertheimer, M. R. *Plasma Processes Polym.* **2004**, *1*, 153.
18. Song, J.; Gunst, U.; Arlinghaus, H. F.; Vancso, G. J. *Appl. Surf. Sci.* **2007**, *253*, 9489.
19. Grill, A. Cold Plasma Materials Fabrication: From Fundamentals to Applications; IEEE Press: Piscataway, New Jersey, **1994**.
20. Grace, J. M.; Gerenser, L. J. *J. Dispersion Sci. Technol.* **2003**, *24*, 305.
21. Hansen, R. H.; Schonhorn, H. *J. Polym. Sci. Part B: Polym. Lett.* **1966**, *4*, 203.
22. Mantell, R. M.; Ormand, W. L. *Ind. Ena. Chem. Prod. Res. Dev.* **1964**, *3*, 300.
23. Schonhorn, H.; Hansen, R. H. *J. Appl. Polym. Sci.* **1967**, *11*, 1461.
24. Pascual, M.; Balart, R.; Sánchez, L.; Fenollar, O.; Calvo, O. *J. Mater. Sci.* **2008**, *43*, 4901.
25. Occhiello, E.; Morra, M.; Cinquina, P.; Garbassi, F. *Polymer* **1992**, *33*, 3007.
26. Mortazavi, M.; Nosonovsky, M. *Appl. Surf. Sci.* **2012**, *258*, 6876.
27. Lee, L. J. *Ann. Biomed. Eng.* **2006**, *34*, 75.
28. Robeson, L. M. *Curr. Opin. Solid State Mater. Sci.* **1999**, *4*, 549.
29. Koros, W. J.; Fleming, G. K.; Jordan, S. M.; Kim, T. H.; Hoehn, H. H. *Prog. Polym. Sci.* **1988**, *13*, 339.
30. Sagle, A. C.; Van Wagner, E. M.; Ju, H.; McCloskey, B. D.; Freeman, B. D.; Sharma, M. M. *J. Membr. Sci.* **2009**, *340*, 92.
31. Hausmann, A.; Sanciolo, P.; Vasiljevic, T.; Weeks, M.; Schroën, K.; Gray, S.; Duke, M. *J. Membr. Sci.* **2013**, *442*, 149.
32. Hassan, A. N.; Anand, S.; Avadhanula, M. *J. Dairy Sci.* **2010**, *93*, 2321.
33. Steen, M. L.; Hymas, L.; Havey, E. D.; Capps, N. E.; Castner, D. G.; Fisher, E. R. *J. Membr. Sci.* **2001**, *188*, 97.
34. Steen, M. L.; Jordan, A. C.; Fisher, E. R. *J. Membr. Sci.* **2002**, *204*, 341.
35. Jokinen, V.; Suvanto, P.; Franssila, S. *Biomicrofluidics* **2012**, *6*, 016501.
36. Steen, M. L.; Butoi, C. I.; Fisher, E. R. *Langmuir* **2001**, *17*, 8156.
37. Tompkins, B. D.; Dennison, J. M.; Fisher, E. R. *Plasma Processes Polym.* **2014**, *11*, 850.
38. Vickerman, J. C. Surface Analysis: The Principal Techniques; Wiley: West Sussex, U.K., **1997**.
39. Mark, J. E., Ed. Polymer Data Handbook; Oxford University Press, Inc.: New York, **1999**.
40. Tompkins, B. D.; Fisher, E. R. *Plasma Processes Polym.* **2013**, *10*, 779.
41. Kosobrodova, E.; Kondyurin, A.; McKenzie, D. R.; Bilek, M. M. M. *Nucl. Instrum. Methods Phys. Res. Sect. B* **2013**, *304*, 57.
42. Larrieu, J.; Held, B.; Martinez, H.; Tison, Y. *Surf. Coat. Technol.* **2005**, *200*, 2310.
43. Larsson, A.; Dérand, H. *J. Colloid Interface Sci.* **2002**, *246*, 214.
44. Morra, M.; Occhiello, E.; Garbassi, F. *Angew. Makromol. Chem.* **1991**, *189*, 125.
45. Murakami, T.; Kuroda, S. I.; Osawa, Z. *J. Colloid Interface Sci.* **1998**, *200*, 192.
46. Greenwood, O. D.; Hopkins, J.; Badyal, J. P. S. *Macromolecules* **1997**, *30*, 1091.
47. Guimond, S.; Wertheimer, M. R. *J. Appl. Polym. Sci.* **2004**, *94*, 1291.
48. Behnisch, J.; Holländer, A.; Zimmermann, H. *Surf. Coat. Technol.* **1993**, *59*, 356.
49. Morra, M.; Occhiello, E.; Gila, L.; Garbassi, F. *J. Adhes.* **1990**, *33*, 77.
50. Trevino, K. J.; Shearer, J. C.; Tompkins, B. D.; Fisher, E. R. *Plasma Processes Polym.* **2011**, *8*, 951.
51. Hofrichter, A.; Bulkin, P.; Drévillon, B. *J. Vac. Sci. Technol. A* **2002**, *20*, 245.
52. Muir, B. W.; McArthur, S. L.; Thissen, H.; Simon, G. P.; Griesser, H. J.; Castner, D. G. *Surf. Interface. Anal.* **2006**, *38*, 1186.
53. Gonzalez, E., II; Barankin, M. D.; Guschl, P. C.; Hicks, R. F. *IEEE Trans. Plasma Sci.* **2009**, *37*, 823.